MODIFICATION OF FATIGUE DAMAGED
STEEL BRIDGE DIAPHRAGMS

By

ADAM BRENT WEST

Bachelor of Science

in Civil Engineering

Oklahoma State University

Stillwater, Oklahoma

1988

Submitted to the faculty of the
Graduate College of
Oklahoma State University
in partial fulfillment of
the requirements for
the Degree of
MASTER OF SCIENCE
July, 1989

MODIFICATION OF FATIGUE DAMAGED

STEEL BRIDGE DIAPHRAGMS

Thesis Approved:

Farel Zwerneman
Thesis Advisor

John P. Lloyd

Rex C. Donahey

Norman N. Durham
Dean of the Graduate College

ACKNOWLEDGEMENTS

I wish to express my sincere appreciation to Dr. Farrel Zwerneman for his guidance and advice throughout my graduate program. I would also like to thank Dr. Rex Donahey and Dr. John Lloyd for serving on my graduate committee. Their suggestions and support were very helpful throughout the research. I would also like to thank Mr. Don Spoonemore for his help and patience while completing my research.

I would like to thank my best friend, Christy Garst, for her encouragement and support throughout my graduate work. Her patience and understanding were without equal.

I would like to acknowledge my parents, Leonda Shields and Ronald West, and the rest of my family, including my brother Eric and my sister Natalie, for their continued support throughout my college education.

TABLE OF CONTENTS

LIST OF TABLES

LIST OF FIGURES

Figure Page

CHAPTER I

INTRODUCTION

1.1 Problem Statement

The Oklahoma Department of Transportation (ODOT) initiated this research soon after an ODOT inspector discovered fatigue cracking in the diaphragms of a steel girder bridge. The bridge, located on I-40 near Weatherford, Oklahoma, is shown in Figure 1. Damage to diaphragms does not pose an immediate threat to the integrity of the bridge; however, loss of the diaphragms will result in loss of support for the concrete deck and possibly accelerate normal deterioration of the deck. In addition, American Association of State Highway and Transportation Officials (AASHTO) specifications require the presence of the diaphragms.

A picture showing several diaphragms is displayed in Figure 2, and two examples of fatigue damage are shown in Figure 3. All cracks initiate at the lower cope, as can be seen in Figure 3, and propagate up through the member. It was found that 40% of the diaphragms have experienced some fatigue damage and five diaphragms have experienced a total section loss. These findings influenced ODOT to initiate research to determine the cause of the cracking and develop solutions for the problem.

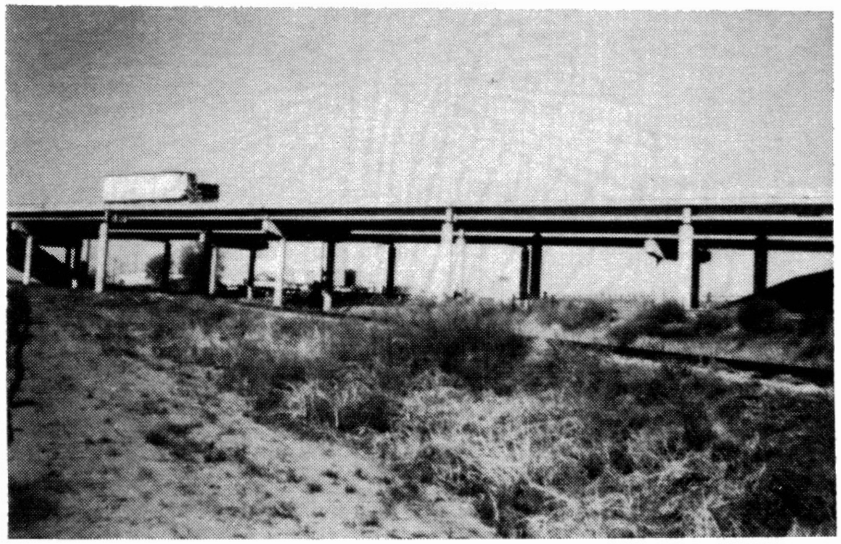

Figure 1. The Bridge With Damaged Diaphragms

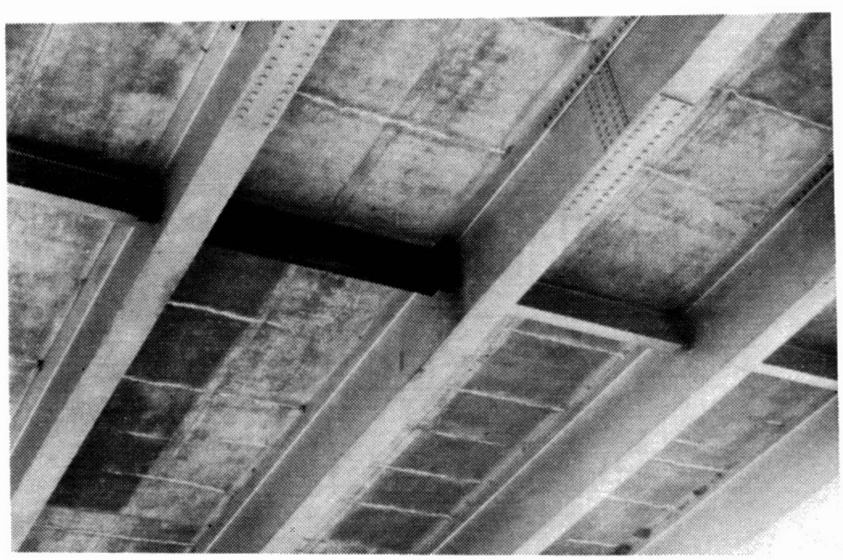

Figure 2. Placement of Diaphragms

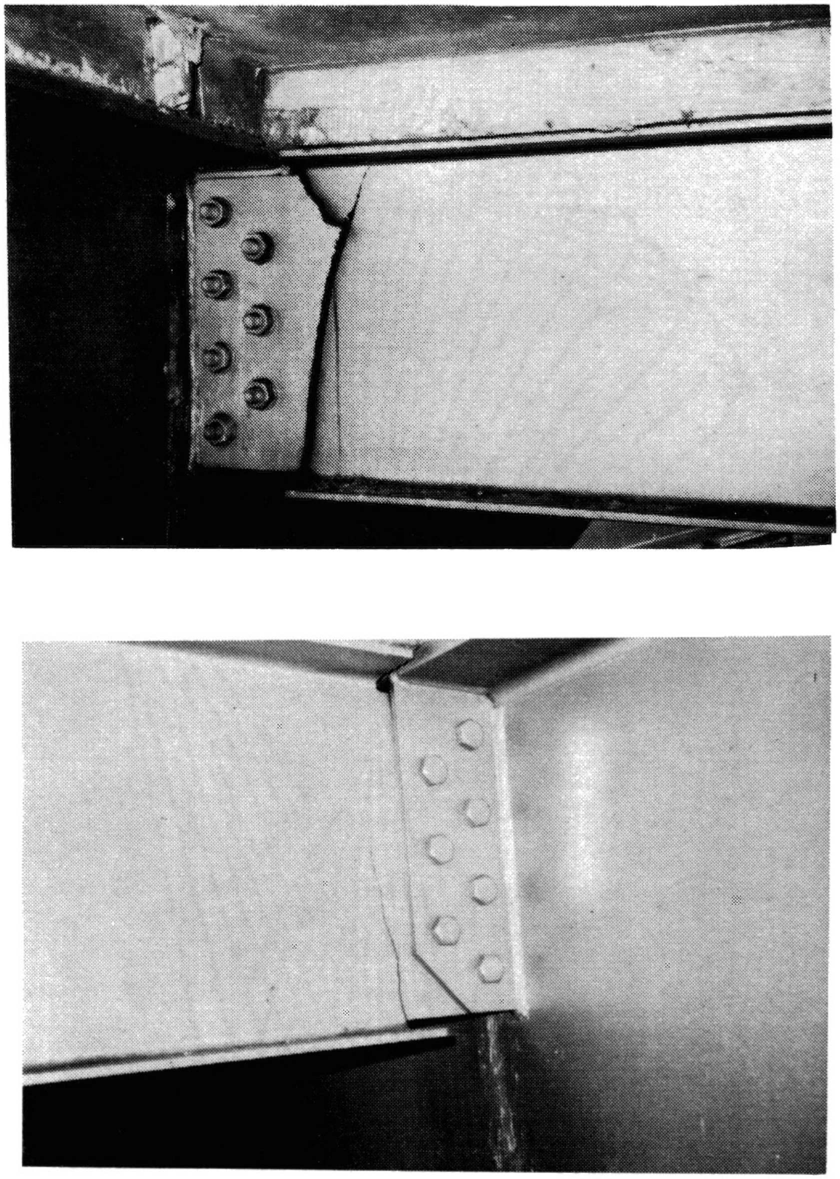

Figure 3. Examples of Diaphragm Cracking

The initial phase of this research, which is not a part of this report, included load testing of the bridge, analysis of the bridge structure, and analytical modeling of the diaphragm. The report containing the initial phase of the research can be found in Reference 9. The phases of the research described within this report consist of a literature review and testing of diaphragms in the laboratory to determine the fatigue life of original and modified details. The literature review is used to acquire some understanding of past bridge fatigue problems and the solutions used in those cases. Laboratory tests allow comparison of fatigue life of the original detail to fatigue life of modified details. Data obtained from laboratory tests will be used as a basis for a solution to the problem.

1.2 Objective of Research

The main objective of this research is to identify a modification which can easily and inexpensively be made to the diaphragms to increase their fatigue life. This will be accomplished by testing the original detail to determine fatigue life and comparing this fatigue life to lives obtained from testing modified members. The modification which possesses the longest fatigue life and is easiest to perform will be selected as the suggested modification.

1.3 Scope of Research

A limited number of modifications will be tested due to time and financial constraints on the project. There are a large number of modifications which could possibly be performed; however, this researcher has concentrated on a small number of the most promising modifications. Modifications are limited to those which can be performed in the field to a structure already in place.

Four modifications were tested in an effort to prove that each of the modifications can increase the fatigue life of the member. It will be shown that removing the bottom two bolts in the connection, welding an auxiliary flange to the web, tapering the cope and the flange, or replacing existing diaphragms with diaphragms not coped at the bottom flange will increase the fatigue life of the member.

The first step in the testing procedure entails designing a loading scheme to approximate the stress distribution found in the member as it exists in the actual structure. The second step is testing the original detail at a variety of stress ranges to develop a plot of stress range versus number of cycles to failure. The modified members were also tested with the same loading apparatus to determine their fatigue lives at a given stress range. These values of fatigue life can then be compared to the data obtained for the original detail to assess the effectiveness of the modification.

CHAPTER II

REVIEW OF LITERATURE

2.1 Damage to Diaphragms and Coped Members

In recent years there has been a large amount of research related to fatigue damage of bridges. There is no doubt that we have a large number of bridges in this country suffering from some failure due to fatigue. A survey conducted between 1978 and 1981 in 20 states and Ontario, Canada, gathered information on 142 bridge sites which had developed some fatigue cracking (2). Out of the 142, 13 of the bridges experienced damage directly related to the diaphragm connection and 13 other bridges experienced damage to coped members. These 26 bridges sustained damage similar to that sustained by the bridge currently being studied.

Aside from the survey above, there are a large number of other cases where coped stringers, floor beams, and diaphragms have experienced fatigue cracks initiating at the lower cope of the flange. At least 30 Japanese railroad bridges developed fatigue cracks at coped flanges of stringers and floor beams, and at least 10 highway bridges have been investigated which have undergone fatigue cracking in a detail similar to the bridge under investigation (2).

One particular case involved Bridge 51.5 of the

Windmere Division of the Canadian Pacific Railroad near Ottawa, Ontario (2). In 1975, seventeen of the coped stringers in the bridge were found to be cracked at the bot-experienced in the bridge. The members were eventually re-paired using the retrofit detail shown in Figure 5. The members in Bridge 51.5 are primary load carrying members, while the members in the bridge currently being investigated are secondary members; therefore, more concern is given to raising the moment capacity of the stringers than the diaphragms of our bridge.

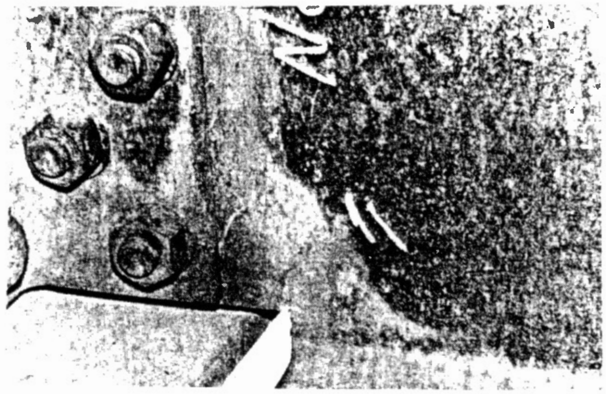

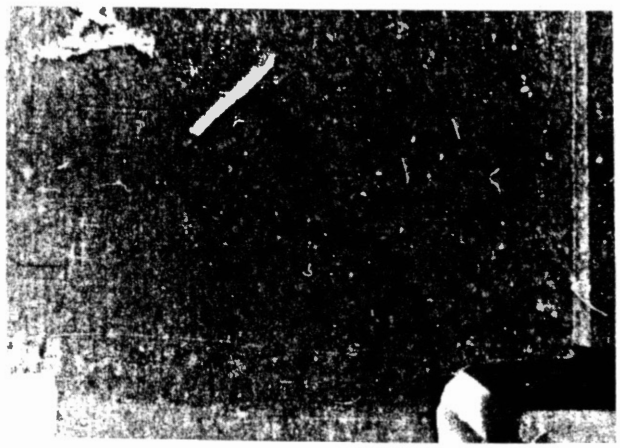

Figure 4. Cracks Found in the Stringer Detail of Bridge 51.5 (2)

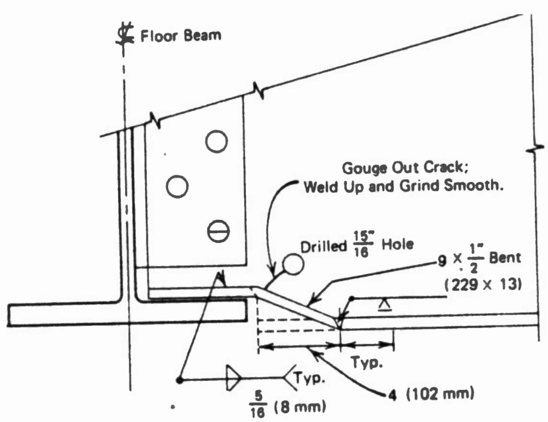

Figure 5. Retrofit Detail Showing Reinforcement of Cross Section (2)

2.2 Modifications to Improve Fatigue Performance

A large amount of the fatigue related material in current AASHTO specifications evolves from the *Bridge Fatigue Guide* (5) by John Fisher. This publication is distributed by the American Institute of Steel Construction (AISC) and covers virtually all areas of design where fatigue damage could be a problem. The publication stresses that "the major factors governing fatigue strength are the applied stress range, the number of cycles, and the type of detail."(5) Unfortunately, when these factors are examined in the context of modifications to secondary members in existing structures, there is no control over the number of cycles and stress range can only be affected by changing the detail. If the fatigue performance of the structure is to be improved, the improvement must come in the form of a more fatigue resistant detail.

The *Bridge Fatigue Guide* offers some recommendations for situations when the lower flange of a diaphragm or stringer must be coped. These recommendations are shown in Figure 6 and Figure 7. It should be noted that the main idea behind each of these modifications is to carry more of the load into the full section and past the coped section of the member where high stress creates difficulties. These modifications are more suited to initial design and construction than repair, but the correction shown in 6b was tested in the current research program.

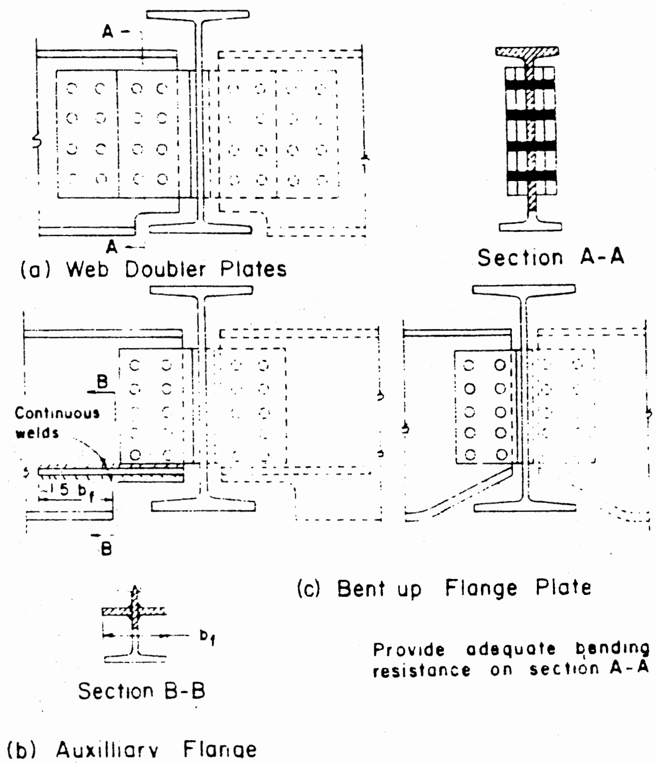

Figure 6. Recommended Connections Where Stringer Flanges Must Clear Floor Beams (5)

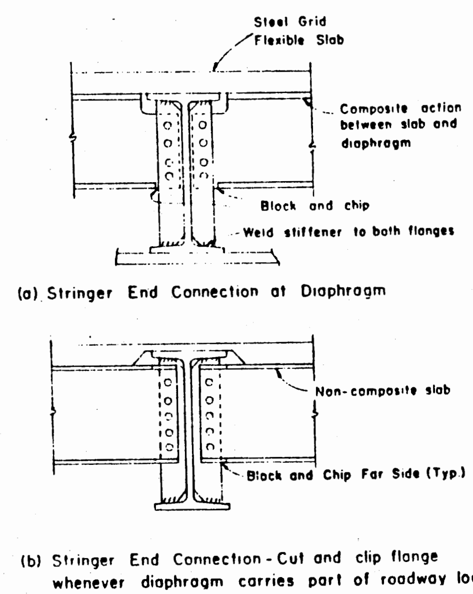

Figure 7. Recommended Treatment at Stringer End Diaphragms (5)

An alternative to carrying the load past the coped section is to smooth out the cope. The major problem with coped members where the cope is in an area of high stress is that this creates a very large stress concentration. The stress concentration can be reduced by creating a more gradual transition into the full section, similar to the transition required at the end of a cover plate (5). The method consists of tapering the cope as shown in Figure 8. In many situations, such as on Bridge 51.5 of the Windmere Pacific Railroad which was mentioned previously, members which have already experienced cracking need to be repaired and reused in the structure. One technique for retarding crack growth is to drill a hole at the end of the crack to reduce the stress concentration. The size of the hole required can be calculated based on the yield stress of the material and the stress intensity factor. Barsom and Rolfe (1) suggest that a fatigue crack will not initiate if

$$\Delta K_I < 5\sigma^{2/3}\rho^{1/2}$$

where σ is the yield stress in ksi,
ρ is the radius of the hole in inches,
ΔK_I is the stress intensity factor in (ksi)(in$^{1/2}$).

Common values used in practice range from 0.5 to 1.0 inch diameter holes (2,4). Drilling holes at the end of cracks is often combined with other methods of repair to produce an efficient and effective retrofitting technique such as that shown in Figure 5.

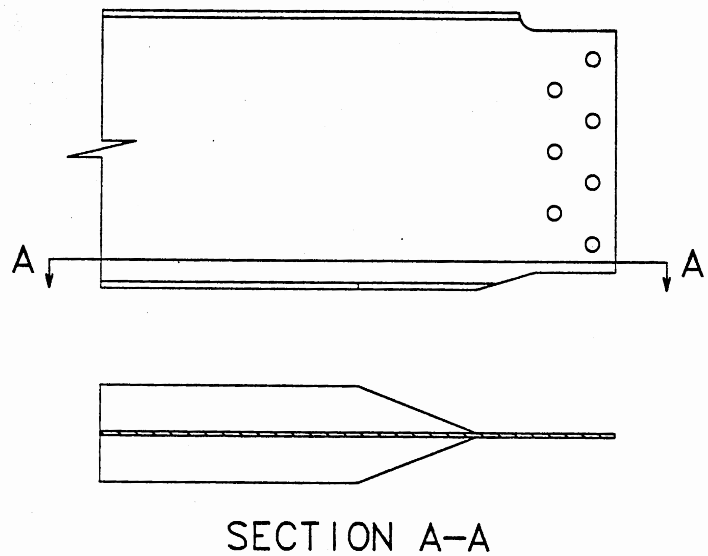

Figure 8. Tapered Cope Detail

CHAPTER III

TESTING EQUIPMENT AND PROCEDURES

3.1 Testing Apparatus

The testing equipment is composed of three main components: structural, hydraulic, and electronic. The structural system supports the test specimen and the hydraulic ram as well as transferring the test loads into the floor system. The hydraulic system supplies the pressure to the ram which applies the load to the specimen. The electronic system controls the application of the loads and monitors the displacements. The testing equipment is shown in Figure 9.

The structural system is composed of two vertical sections and a wide flange connecting the vertical members. The vertical members provide support for the ram and specimen as well as transferring the test load into the floor system. The horizontal member adds rigidity to the system, provides upward support for the ram and specimen, and is used to help prevent lateral displacements of the specimen. The role of preventing lateral displacements will be discussed in more detail in the next section.

The electronics and hydraulics function as a closed loop servo-controlled system. The electronics system includes a function generator to produce a sinusoidally varying load time history and a peak detector to monitor the applied load. Load is applied through a 50 kip capacity hydraulic ram.

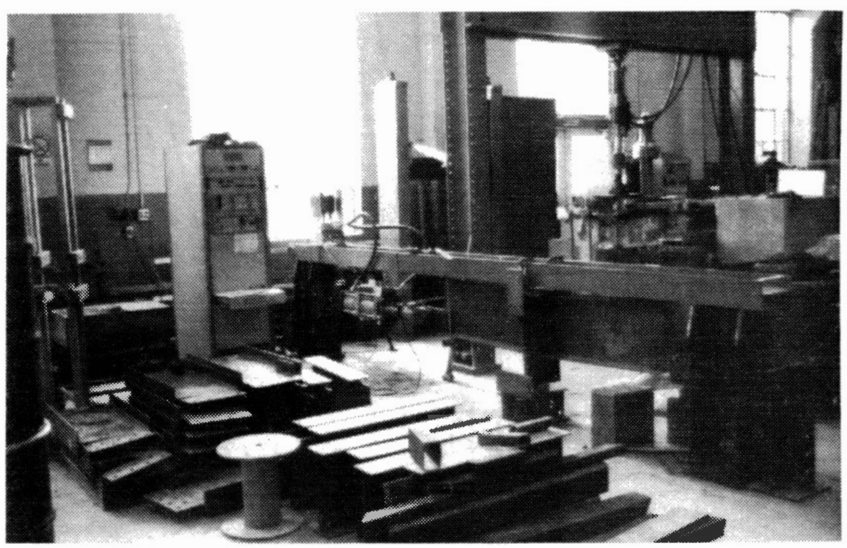

Figure 9. Testing Equipment

3.2 Loading Scheme

Field measurements and analytical investigation show that the diaphragms are acting compositely with the concrete deck. The neutral axis for the composite beam was found to occur near the top flange of the steel diaphragm. It was decided that the simplest way to reproduce the stress distribution found in the field was to apply an eccentric tensile load to the laboratory specimen. The eccentricity was set so that the stress due to bending and the stress due to tensile load combine to create the desired stress distribution. Calculations of eccentricity are shown in Appendix A, and the resulting test specimen is shown in Figure 10.

The loading scheme is designed to test two specimens at one time by connecting them to a simulated girder as shown in Figure 11. The girder has the same flange width and the same size gusset plate as the actual girder on the bridge; therefore, the connection is a very good simulation of the connection on the bridge.

One problem that arose during the initial test was a large lateral displacement which occurred when load was applied to the specimen. During cyclic loading, the specimen became laterally unstable. This problem was solved by attaching restraints to the simulated girder which do not allow lateral motion but do allow vertical and longitudinal motion. The restraints, which are shown in Figure 12, bolt

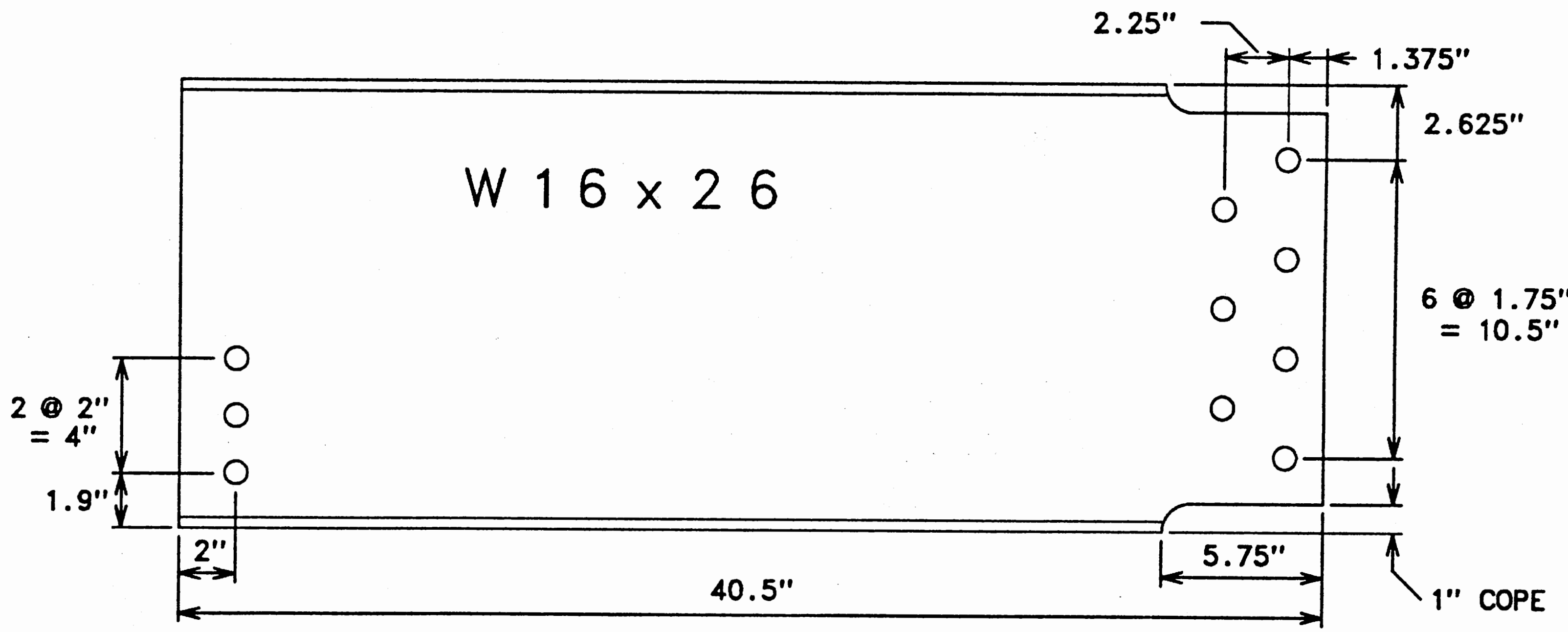

NOTE: ALL HOLES HAVE A DIAMETER OF 13/16 INCHES.

Figure 10. Test Specimen for Original Detail

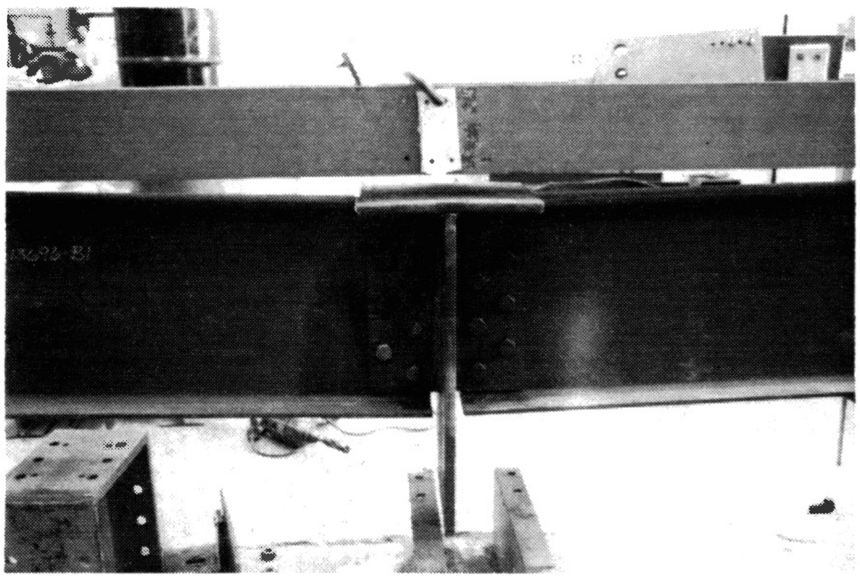

Figure 11. Simulated Girder

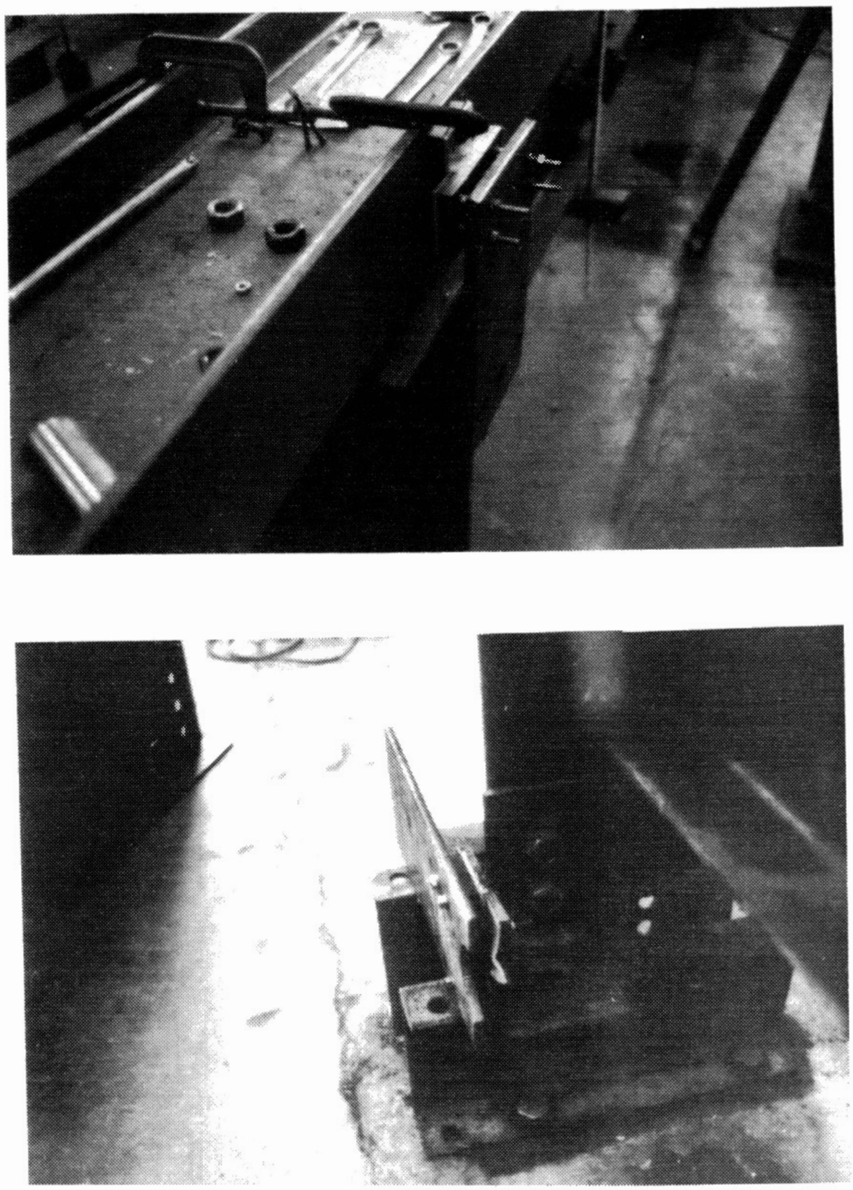

Figure 12. Lateral Restraints

to the girder in three locations: the upper web on both ends of the girder and the lower web on one end of the girder. Each restraint uses two Teflon pads which are able to slide freely against one another in the desired direction of motion. Each restraint uses one pad connected to the girder and a second pad attached to a stable surface. The stable surface for the top two restraints is the structural wide flange, and the stable surface for the lower restraint is a floor attachment. The restraints perform adequately to resist the undesirable motion. It should be noted that the problem with lateral motion does not occur on the bridge because the diaphragms are connected to a stiff longitudinal girder.

3.3 Application of Loads

As was stated earlier, stress range is one of the most important factors governing fatigue life; therefore, the cyclic loads must be applied at magnitudes which correspond to known stresses in the specimen. Since the electronics control application of the sinusoidal cyclic loads, we only need to calculate the maximum and minimum loads required to cause a known stress range in the specimen. The ratio of minimum load to maximum load was held constant at 0.15. Calculations of loads are demonstrated in Appendix B, and the values are shown in Table 1.

TABLE 1

LOADS USED AT SPECIFIED STRESS RANGES

Load, kips			Nominal
Max.	Min.	Load Range, kips	Stress Range, ksi
29.41	4.41	25	20
23.53	3.53	20	16
17.65	2.65	15	12
11.76	1.76	10	8

3.4 Failure of Members

During the initial test, it became apparent that it is not practical to allow the tests to run until the crack had propagated completely through the section because of possible damage to the testing equipment. However, after the crack has propagated through approximately half of the diaphragm, a relatively insignificant number of cycles remain until complete failure of the cross section. Therefore, test specimens are considered to be failed when the crack has propagated into the upper half of the diaphragm.

3.5 Modifying the Diaphragm

All of the modifications to improve fatigue life were carried out using an oxyacetylene torch, a magnetic based drill, a band saw, an arc welder, and a hand grinder. Only a nominal amount of experience is required to perform the operations. Specific modifications are described in detail in the following chapter.

CHAPTER IV

DISCUSSION OF RESULTS

4.1 Analysis Of Original Detail

4.1.1 Comparison of Experimental Stress Distribution to the Actual Stress Distribution

To help verify the loading scheme, a lab specimen was instrumented with 45 degree strain rosettes, and strain readings were taken. The positions of the rosettes are approximately the same as the rosettes applied to the actual structure. The positions of the strain rosettes are shown in Figure 13. The strains obtained from loading the lab specimen were converted to principal stresses as shown in Appendix C, and the stress distribution is plotted in Figure 14. The neutral axis of the actual bridge member is located above the flange due to composite action with the slab. The position of the neutral axis is shown in Appendix A. The position of the neutral axis in the laboratory tests very closely agrees with that of the actual structure. A thorough examination of the stresses in the bridge is contained in Reference 9, and comparison indicates that approximately the same stress distribution occurs. The presence of approximately the same stress distribution in the lab and in the actual structure gives credibility to the loading scheme being used.

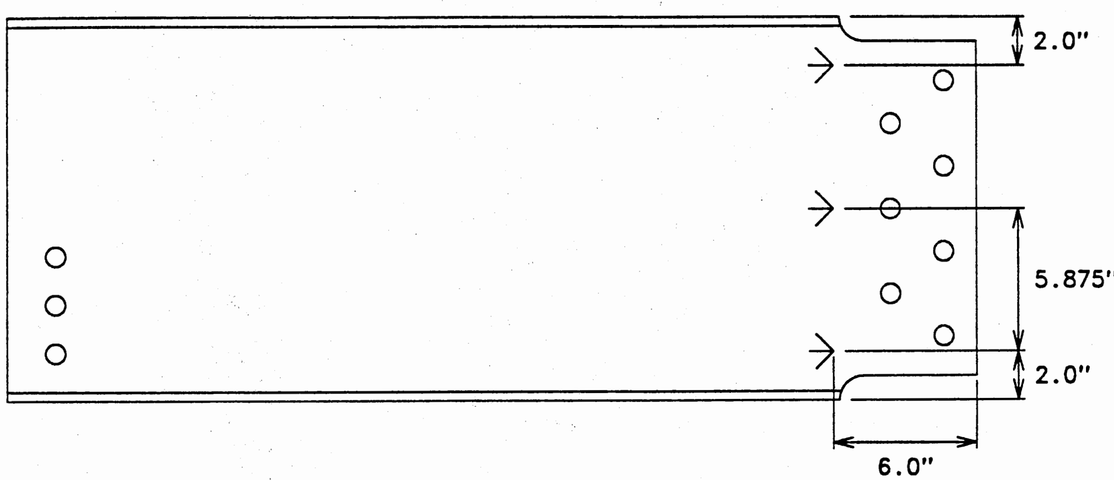

Figure 13. Position of Strain Rosettes

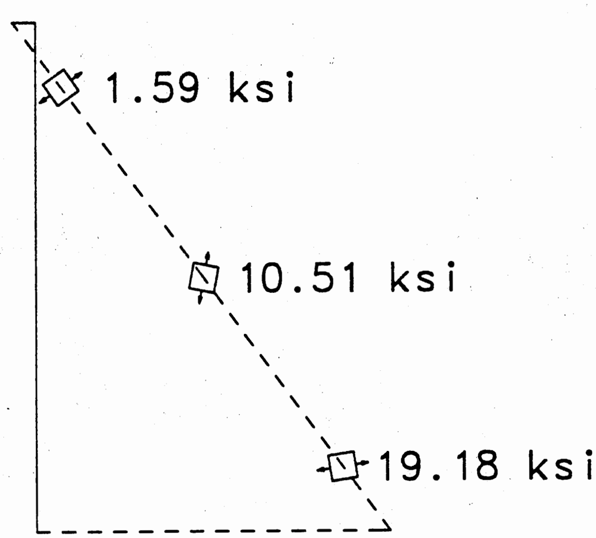

Figure 14. The Laboratory Distribution of Principal Stesses

4.1.2 Comparison of Cracking Patterns

Typical cracking patterns of the lab specimens are shown in Figure 15. These patterns are very similar to those found in actual bridge members which are shown in Figure 3. The similarities between these two cases help to verify the laboratory model.

4.1.3 Fatigue Life of Original Detail

The original detail was tested at a variety of stress ranges to obtain a plot which is representative of its fatigue life. The data obtained are shown in Table 2, and a plot is shown in Figure 16. A line was fit to the data using the least squares method, and the equation is shown on the plot. Data for tests discontinued without failure were not included in the regression line. The 90% confidence limit lines shown in the plot indicate that there is a 90% probability that future values would fall within the limits. The data obtained and the resulting fitted line are very much what would be expected from a fatigue test of this kind and are a good basis from which to compare modifications. The detail can be placed in a specific stress category as discussed in Reference 5. The fatigue data is plotted in Figure 17 with the corresponding stress category superimposed to show that the detail is a category D detail.

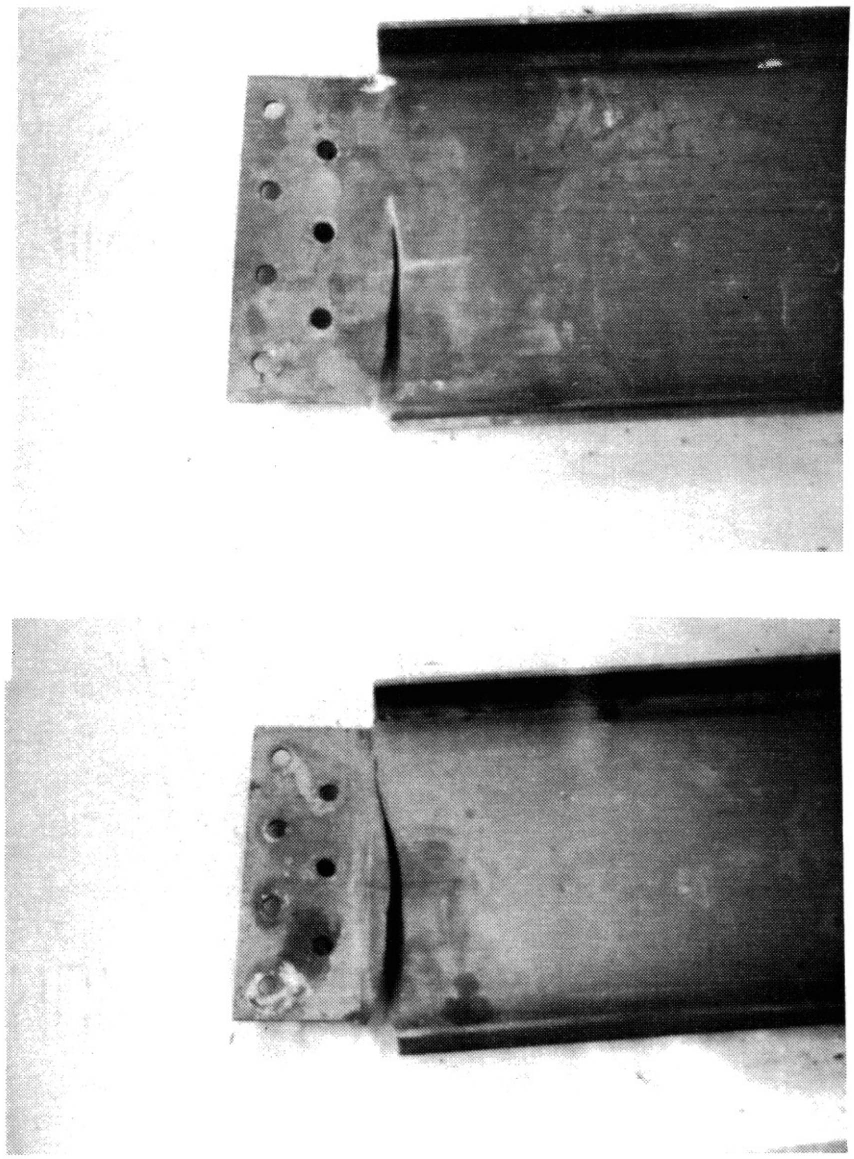

Figure 15. Typical Cracking Pattern in Laboratory Specimen

TABLE 2

FATIGUE LIFE OF ORIGINAL DETAIL

Stress Range, ksi	Number of Cycles to Failure
20	195160
	240740
16	529660
	835220
12	1213240
	1431580
8	6824790 *
	6824790 *

* Tests were discontinued.

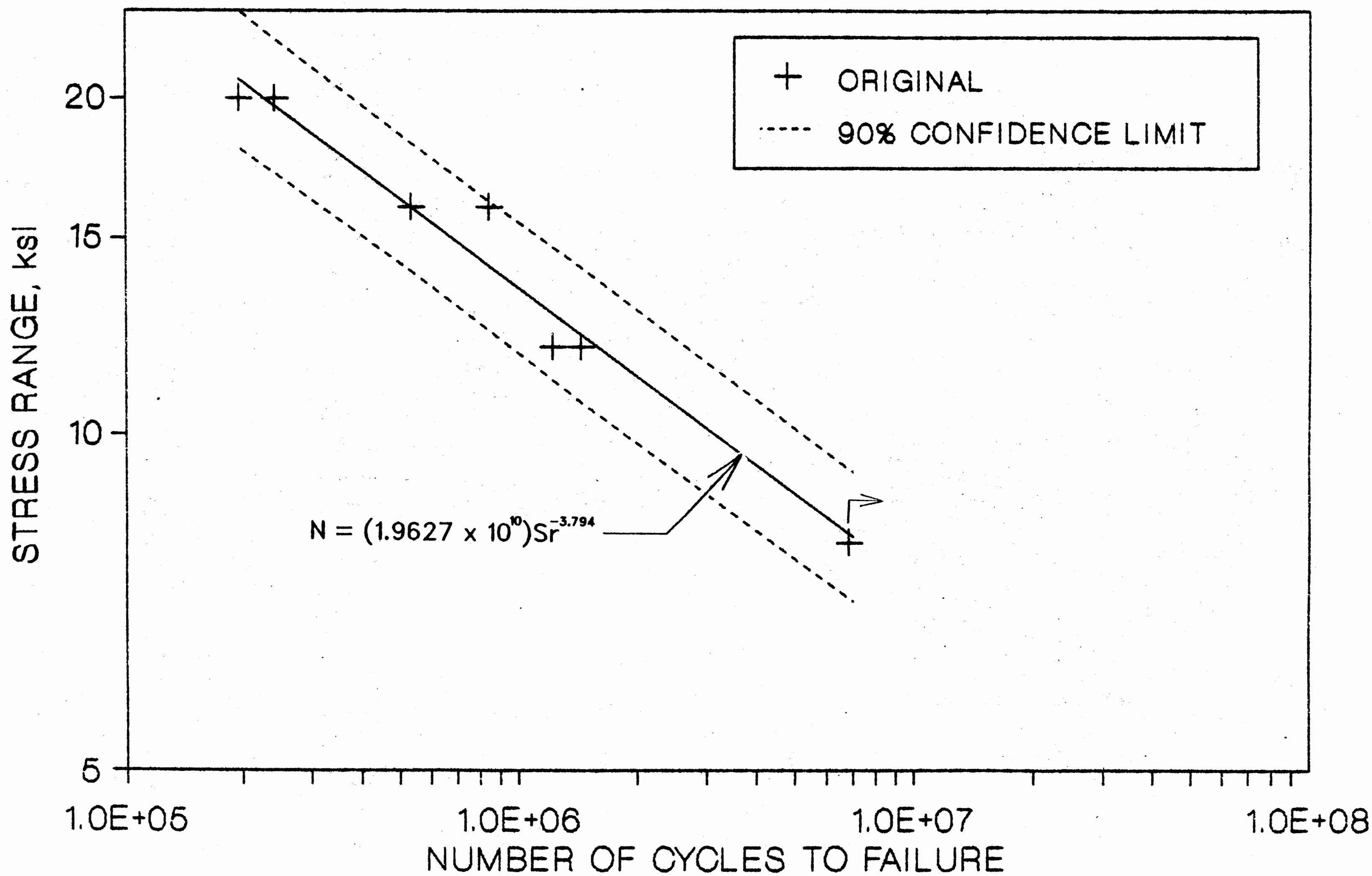

Figure 16. Fatigue Life of Original Detail

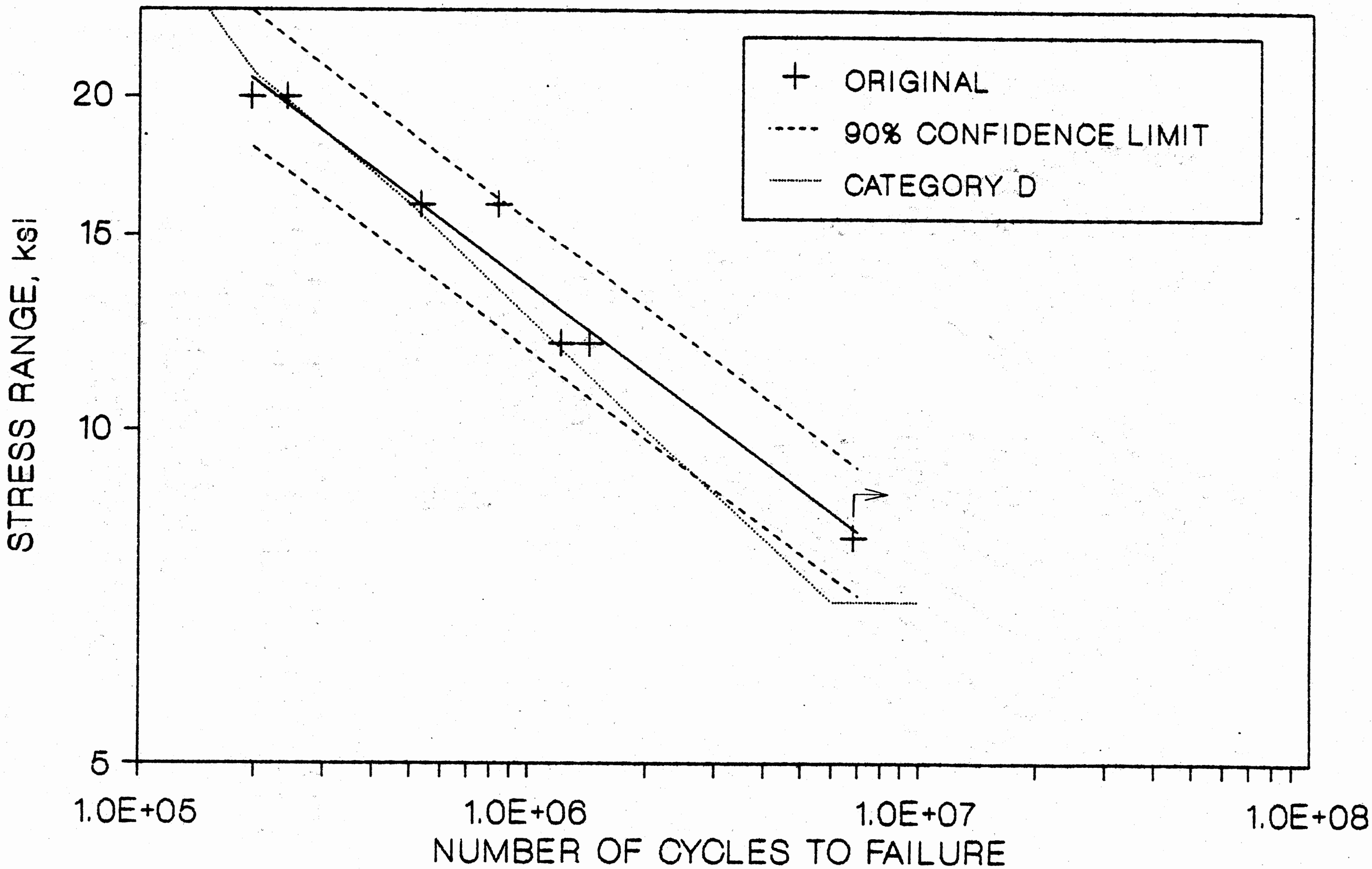

Figure 17. Fatigue Life of Original Detail Compared to a Category D Detail

4.2 Comparison of the Original Detail to Modified Detail

4.2.1 Modifications Tested

Four modifications to the original detail were tested. The first modification consists of simply removing the two bottom bolts in the connection. The second modification involves welding an auxiliary flange to the web of the diaphragm as shown in Figure 18. The third modification is carried out by tapering the cope as shown in Figure 19. The fourth modification is only for replacement purposes and requires installing a new diaphragm without a bottom flange cope.

4.2.2 Removal of the Two Lower Bolts

Removal of the two lower bolts relieves the stress at the lower cope while leaving the connection with enough capacity to carry the wheel loads of an H20 truck as shown in Appendix D. The stress distribution of the member is shifted upward in comparison to the original, as shown in Figure 20. Figure 21 shows that, in addition to the stress reduction, the direction of the principal stress is rotated slightly to the vertical in comparison to the original.

The drastically reduced stress at the lower cope and the angle on which the principal stress acts reduces the possibility that a fatigue crack will propagate from the lower cope, and as a result, the fatigue life of the member is increased. The experimental values for fatigue life are shown in Table 3 and are plotted against the original detail life in Figure 22.

Failure in this modified detail occurred when a crack initiated in one of the bolt holes and propagated through the web as shown in Figure 23. Crack growth did not originate in the cope. Removal of the bottom bolts resulted in an increased eccentricity of the load relative to the connection. High loads on the lowest remaining bolt caused a bearing failure in the diaphragm which contributed to crack initiation in this area. On the bridge, this increase in eccentricity should not occur, and the loads at the bottom bolts will be much less.

Tests were also conducted with specimens which were allowed to crack approximately one inch prior to removing the bolts. The tests were continued with the bolts removed. The cracks did not propagate, and the failure occurred through the bolted connection. This indicates that when relatively short cracks are present, removal of the bottom two bolts can hinder further propagation.

The results from these tests are consistent with the theoretical results found in Reference 9.

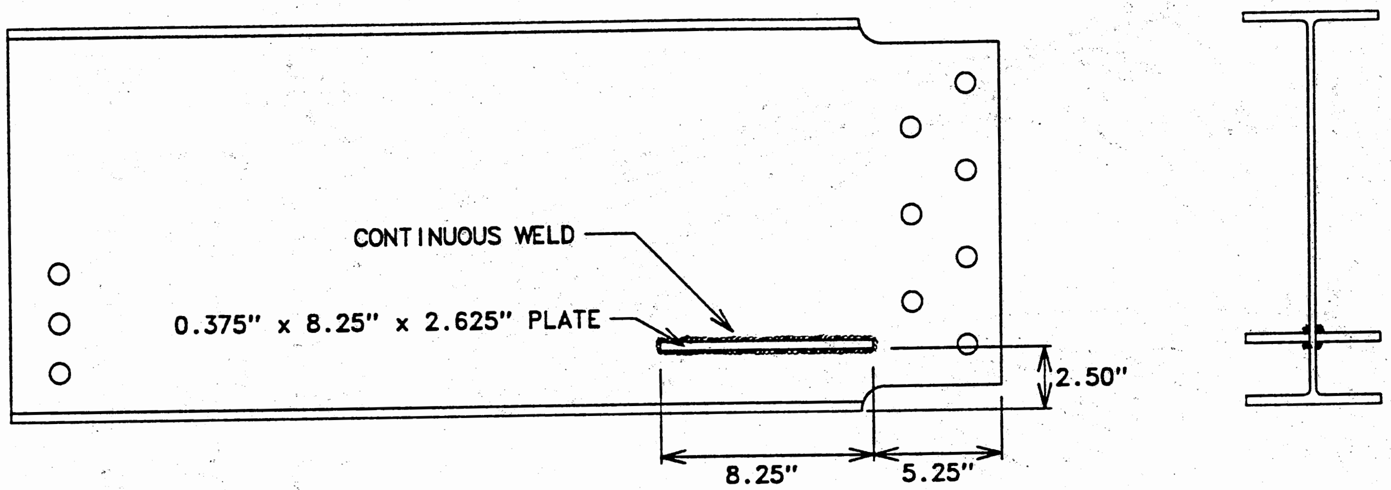

Figure 18. Auxiliary Flange Detail

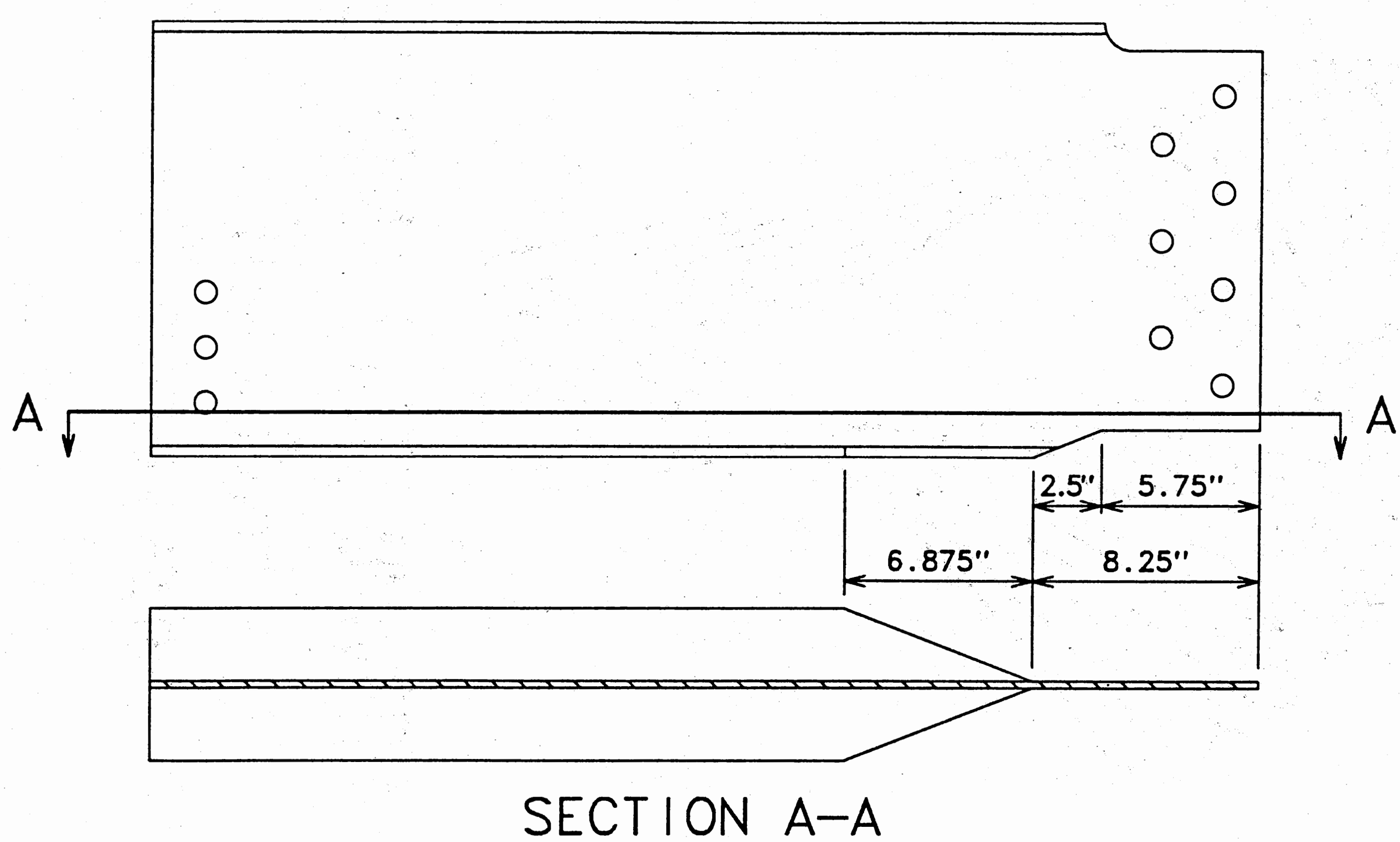

Figure 19. Tapered Cope Detail

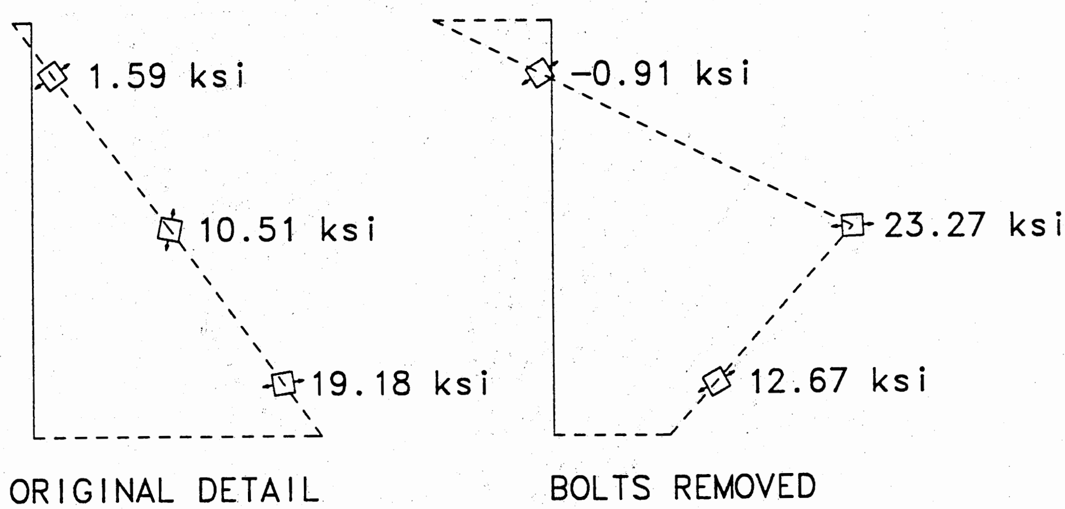

Figure 20. Comparison of Principal Stresses of Original Detail to Detail With Bolts Removed

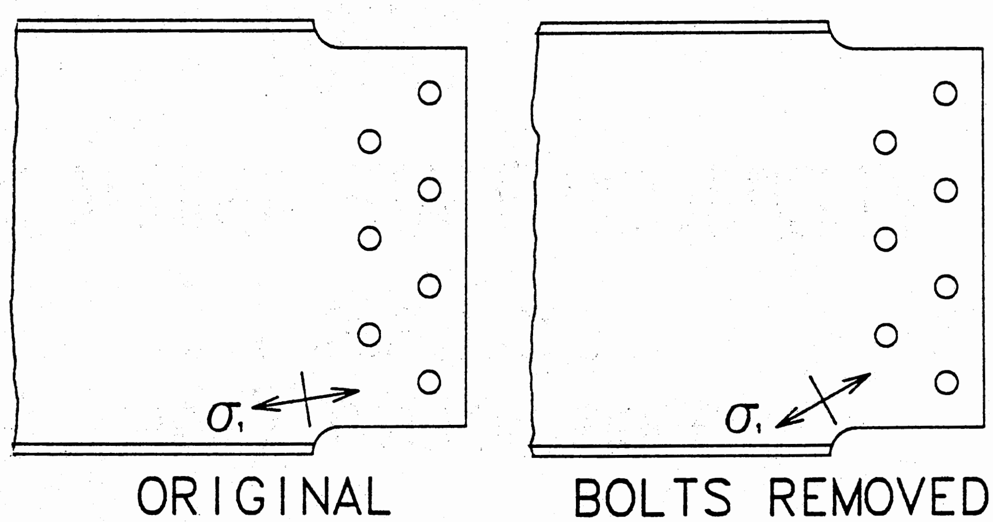

Figure 21. Comparison of Direction of Principal Stress of Original Detail to Detail With Bolts Removed

TABLE 3

FATIGUE LIFE OF MODIFICATIONS

Modification	Number of Cycles to Failure for 20 ksi Stress Range
Two lower bolts removed	1188380
	547730
Auxiliary Flange	360940
	1790810
Tapered Cope	656590
	2066660
New member with no cope	2788480 *
	2001970 *

* Test was discontinued.

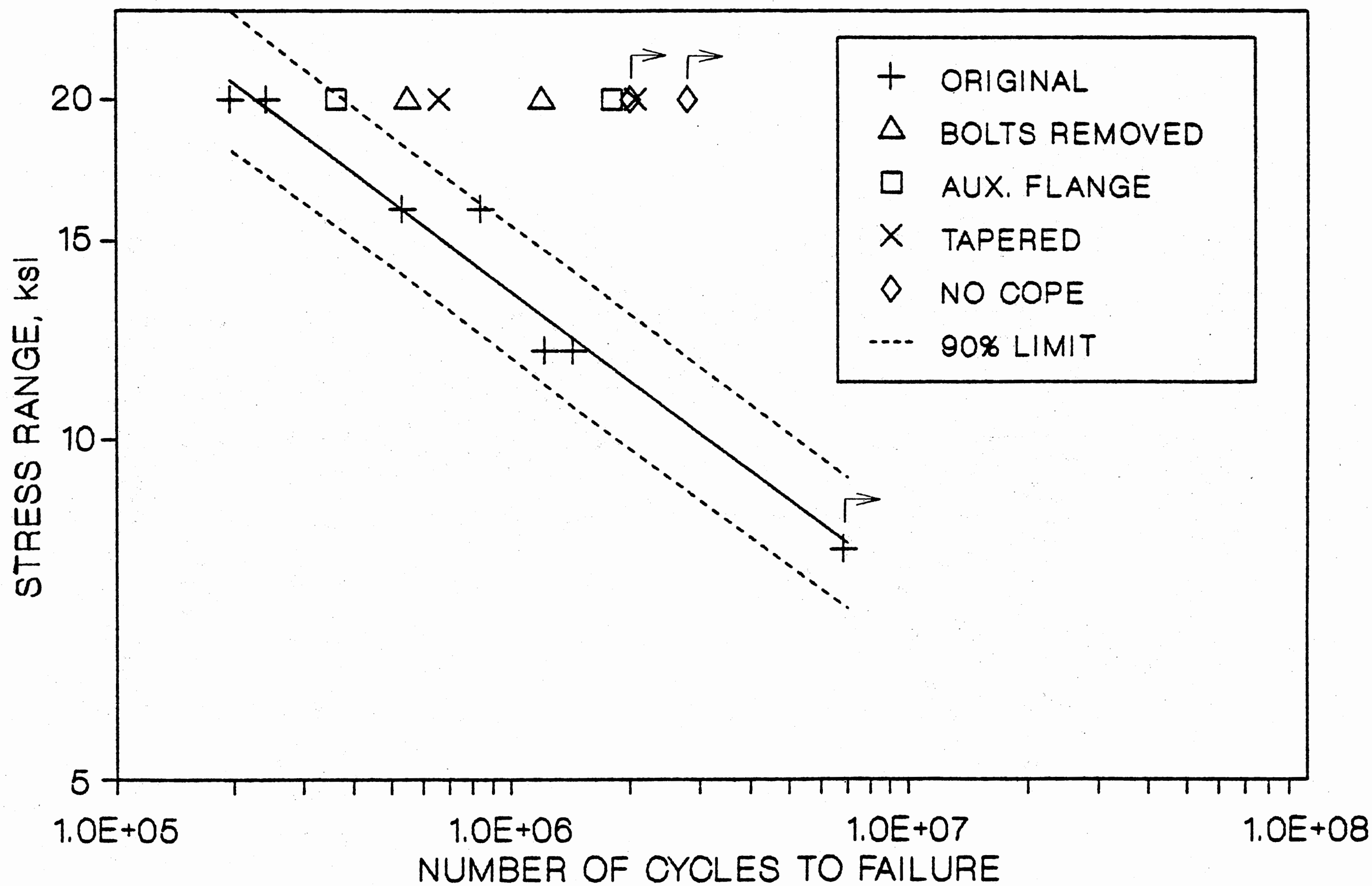

Figure 22. Fatigue Life of All Specimens

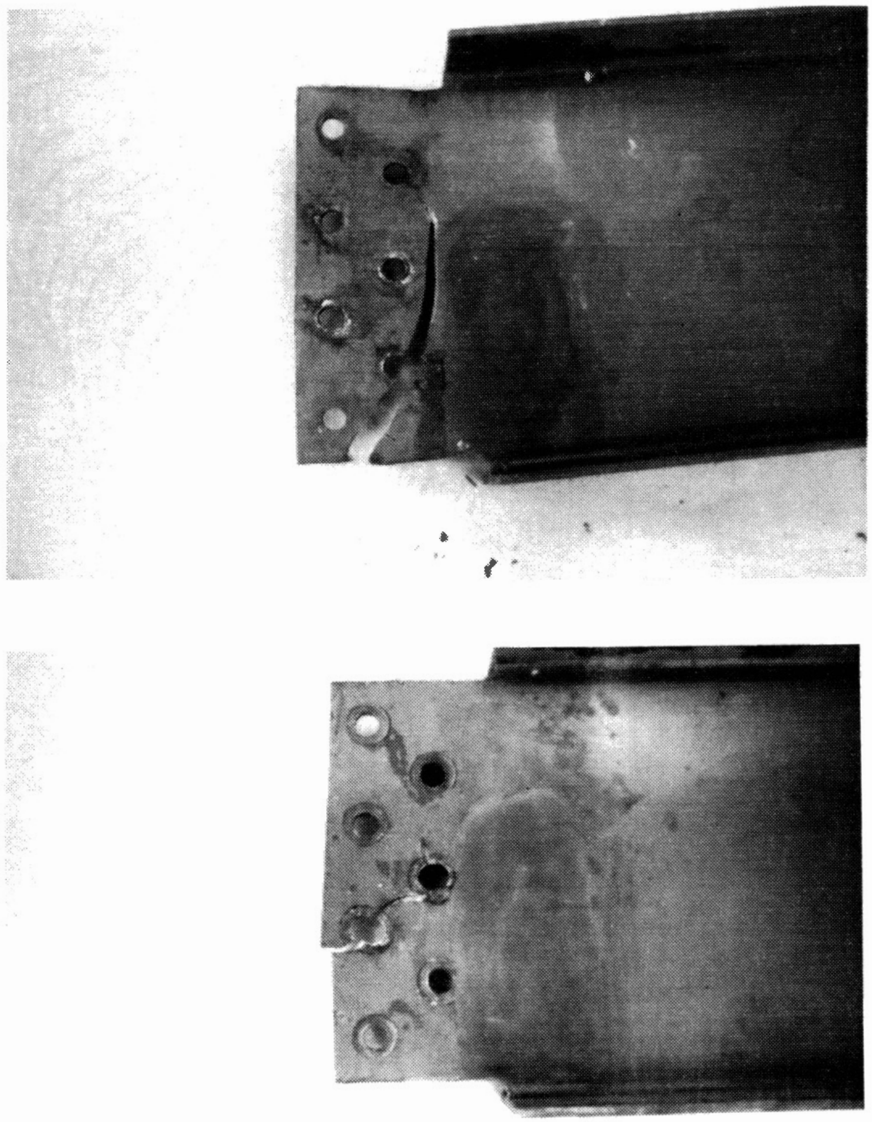

Figure 23. Failure of Detail With Bolts Removed

4.2.3 Auxiliary Flange Detail

The auxiliary flange is installed to carry a portion of the load past the cope and reduce the stress in this area. A problem with applying this technique to the current situation is that the gusset connection does not allow the auxiliary flange to extend ahead of the cope far enough to help relieve a large portion of the stress.

The tests with the auxiliary flange were conducted on specimens having fatigue cracks which had already propagated approximately 3/4 of an inch prior to any modifications being performed. This was done as a worst case for any situation in which this modification might be used. A 1/2 inch diameter hole was drilled at the end of the crack to help retard crack growth. This hole size was selected to match the size web in Reference 4. The auxiliary flange was then welded on as previously shown in Figure 18.

The fatigue life of the specimen was not significantly increased by performing this procedure, as can be seen in Table 3 and Figure 21. The crack continued to propagate after a short period of no growth and cracked around the edge of the auxiliary flange, as shown in Figure 24. The fact that the crack easily propagated around the auxiliary flange is another indicator that the flange does not extend far enough ahead of the cope to be effective.

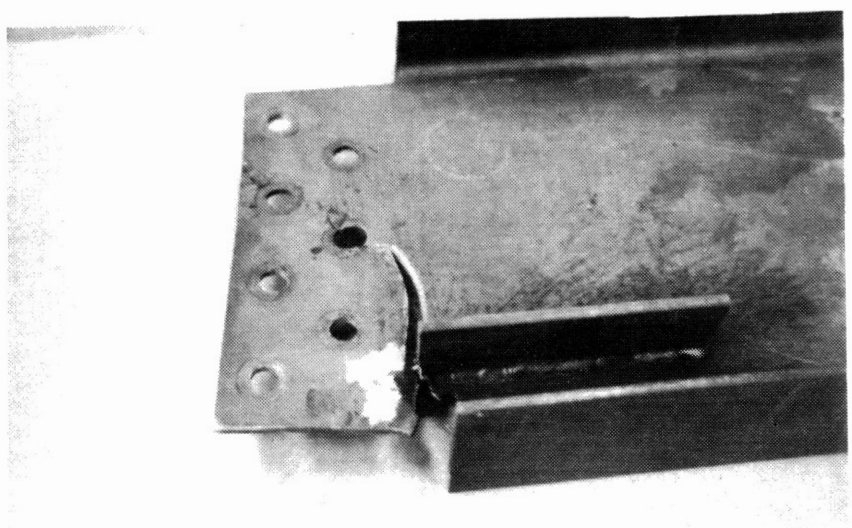

Figure 24. Failure of the Auxiliary Flange Detail

4.2.4 Tapered Cope Detail

The fatigue life of the tapered cope detail was very dependent on how carefully the cutting and grinding procedures were carried out. As can be seen in Table 3 and Figure 21, the tests resulted in a wide disparity of fatigue life for the detail. One test resulted in a very good increase while another test resulted in a minimal increase.

Reference 9 suggests that the tapered cope detail exhibits virtually no decrease in stress concentration when compared to the original detail. The cracking pattern for this detail, which is shown in Figure 25, also behaves very similarly to that of the original detail. All of these facts indicate the tapered detail does not make a consistent and significant improvement over the original detail.

4.2.5 Uncoped Detail

The uncoped detail was tested to establish that an uncoped member will not have the problems associated with the coped members. All of the specimens underwent approximately 2 million cycles and never failed in any way. The data is shown in Table 3 and in Figure 22.

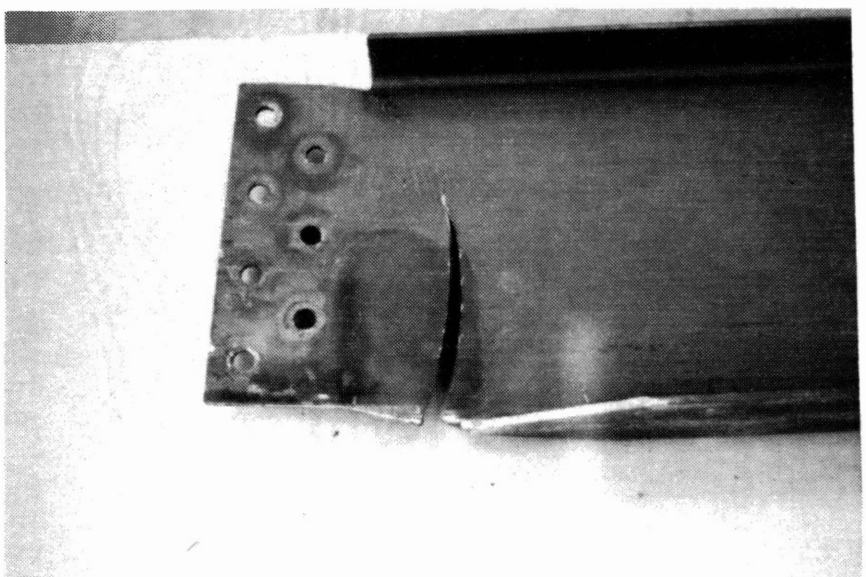

Figure 25. Failure of Tapered Cope Detail

CHAPTER V

SUMMARY AND CONCLUSIONS

The objective of this research is to identify a modification which can easily and inexpensively be made to the diaphragms to increase their fatigue life. To solve this problem, literature concerning past cases of fatigue damage and current specifications were reviewed to determine what steps should be taken. Four modifications were selected to be tested. The fatigue lives of the original detail and these four modifications were determined through laboratory testing. The fatigue lives of the modifications were compared to the life of the original detail and to the lives of the other modifications. Other considerations such as changes in stress distribution were also analyzed.

The recommendations include two possible solutions. The first solution is to remove the bottom two bolts from the connection for the members which have not cracked or which have experienced minimal cracking less than approximately one inch. The second solution is to use uncoped diaphragms to replace all members which have experienced cracking in excess of approximately one inch.

A SELECTED BIBLIOGRAPHY

1. Barsom, J. M., and Rolfe, S. T., "Fracture and Fatigue Control in Structures." *Application of Fracture Mechanics,* Prentice-Hall, Inc., 1987, pp 262.

2. Fisher, J. W., "Fatigue and Fracture in Steel Bridges.", Wiley-Interscience, New York, 1984, pp 302-310.

3. Fisher, J. W., et al., "Fatigue of Welded Steel Bridge Members Under Variable Amplitude Loadings", NCHRP Report 188, 1978.

4. Fisher, J. W., et al., "Detection and Repair of Fatigue Damage in Welded Highway Bridges", NCHRP Report 206, 1979.

5. Fisher, J. W., "Bridge Fatigue Guide, Design and Details", American Institute of Steel Construction, 1977.

6. Fisher, J. W., et al., "Review of Field Measurements for Distortion Induced Fatigue Cracking in Steel Bridges", Transportation Research Board, Record 1118.

7. Gere, James M., and Timoshenko, Stephen P., "Mechanics of Materials", 2nd ed., PWS Publishers, Boston, 1984.

8. Keating, Peter B., and Fisher, John W., "Fatigue Behavior of Variable Loaded Bridge Details Near the Fatigue Limit", Transportation Research Board, Record 1118.

9. Lim, Kee Seong, "Fatigue Damage to Steel Bridge Diaphragms, Field Investigation", Master's Thesis, Oklahoma State University, School of Civil Engineering, May,1989.

10. "Manual of Steel Construction, Load and Resistance Factor Design", American Institute of Steel Construction, 1986.

11. "Student Manual for Strain Gage Technology", Micro-Measurements Division, Measurements Group, Inc., 1978.

APPENDIX A

CALCULATION OF LOAD ECCENTRICITY

The necessary eccentricity can be calculated by determining the desired stress distribution. Figure 26 shows the composite section of the diaphragm and the slab. The calculation of the position of the neutral axis is shown below.

The Neutral Axis

effective width = length / 8 = 4 (8.5') / 8 = 51 inches

$$c = \frac{(51''/8)(7.5'')(-7.5''/2) + (7.68\ in^2)(15.69''\ /\ 2)}{(51''/8)(7.5'') + (7.68\ in^2)}$$

c = -2.15"

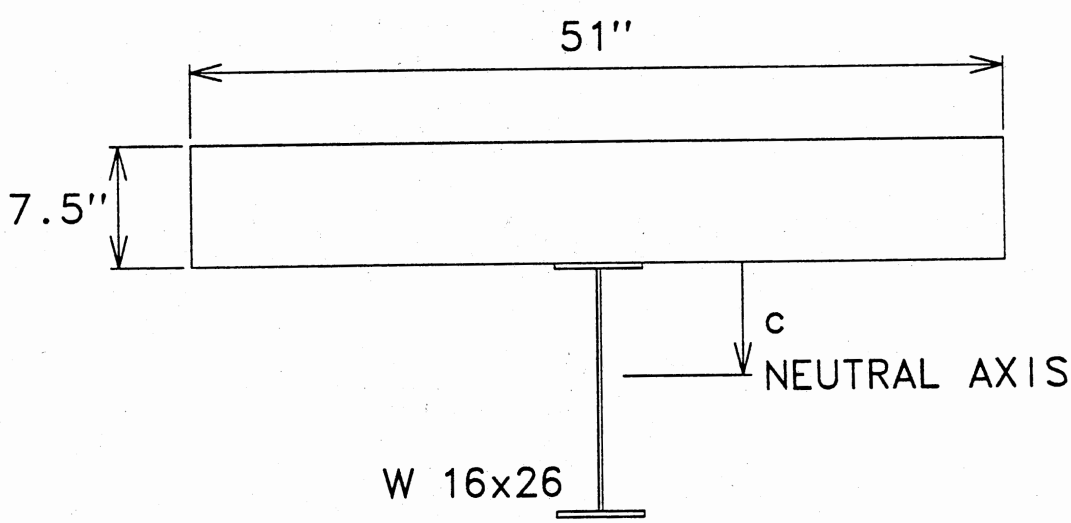

Figure 26. Composite Section

The eccentricity can now be calculated by assuming the stress distribution shown in Figure 27 and calculating the position of the axial load required to cause the distribution.

Calculation of Eccentricity

$$\sigma = \frac{P}{A} + \frac{Pey}{I} \qquad @ \text{ N.A. } \sigma = 0 \quad y = -10$$

$$0 = \frac{1}{7.68 \text{ in}^2} + \frac{e(-10'')}{301 \text{ in}^4}$$

Solving for e

$e = 3.92''$

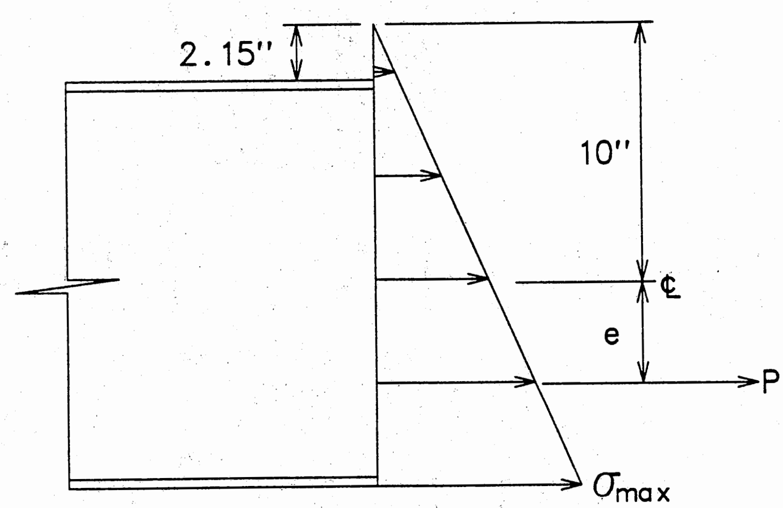

Figure 27. Stress Distribution and Eccentricity of Applied Load

APPENDIX B

CALCULATION OF APPLIED LOADS

The relationship between the applied load and the nominal stress at the lower fiber is calculated as shown below.

<u>Section Properties</u>

Area = (13.625")(0.25") = 3.41 in^2

I = (b)(h^3)/12 = (.25)(13.625)^3/12 = 52.69 in^4

<u>Relationship for σ_{max}</u>

$$\sigma_{max} = \frac{P}{A} + \frac{Mc}{I} = \frac{P}{3.41\ in^2} + \frac{P(3.92")(\frac{13.625"}{2})}{52.69\ in^4}$$

$$\sigma_{max} = (0.8\ \ in^{-2})P$$

or

$$\Delta P = (1.25\ \ in^2)\,\sigma_{range}$$

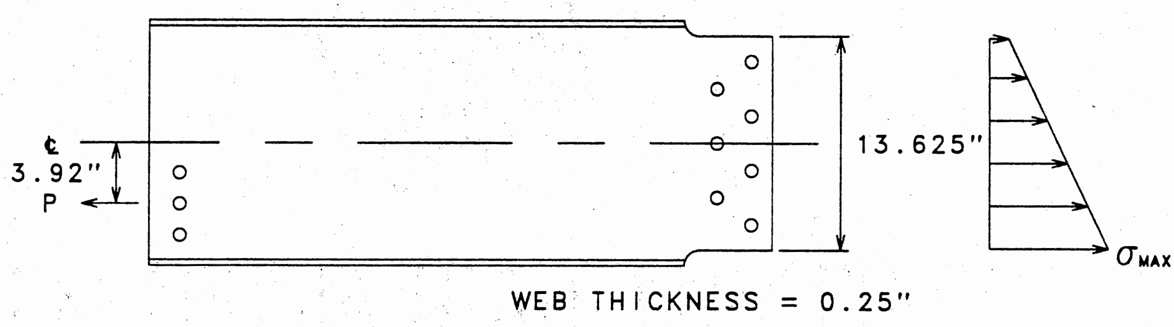

Figure 28. Section With Stress Distribution

Maximum and minimum loads were set so that P_{min}/P_{max} = 0.15 for all load ranges. This relationship simplifies to yield: P_{max} = ΔP / 0.85 and P_{min} = P_{max} - ΔP. In this way, load ratio was removed as a variable in the tests.

The relationships can be combined to form the following two relationships: $P_{max} = (1.4706)\sigma_{range}$, $P_{min} = (0.2206)\sigma_{range}$. For the stress range of 20 ksi we can calculate the loads as shown below.

$$P_{max} = (1.4706\ in^2)(20\ ksi) = 29.41\ k$$

$$P_{min} = (0.2206\ in^2)(20\ ksi) = 4.41\ k$$

The remainder of the values are shown in Table 4.

TABLE 4

LOADS USED AT SPECIFIED STRESS RANGES

Load, kips			
Max.	Min.	Load Range, kips	Nominal Stress Range, ksi
29.41	4.41	25	20
23.53	3.53	20	16
17.65	2.65	15	12
11.76	1.76	10	8

APPENDIX C

CALCULATION OF STRESSES

Strain Rossettes were placed on a test secimen, and reading were taken with a 30 kip load applied. The readings were taken twice each for two cases: the original detail and the original detail with the two bottom bolts removed. The gages were numbered as shown in Figure 29, and the average strain reading is shown for each case in Table 5.

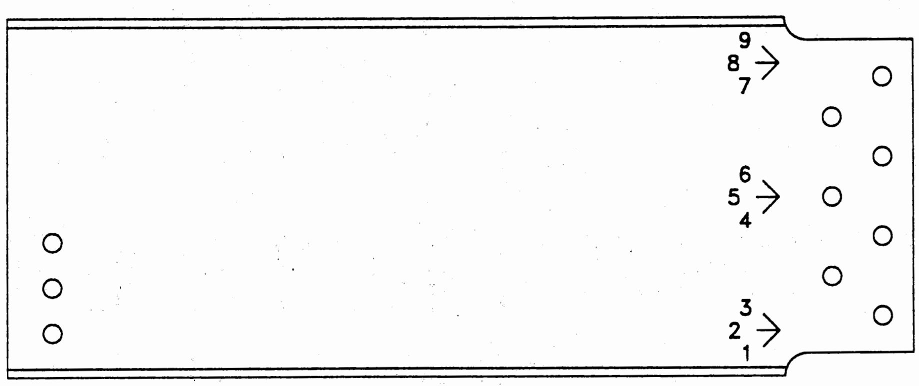

Figure 29. Numbering of Strain Gages

TABLE 5

STRAIN READINGS

Rosette	Gage	Strain x 10^6	
		Original	Bolts removed
1	1	393.5	389.5
	2	601.0	307.5
	3	193.5	-62.5
2	4	72.5	434.5
	5	335.0	712.0
	6	221.0	365.0
3	7	-155.0	-410.5
	8	-75.5	-290.0
	9	89.0	67.5

The strain readings can be converted to stresses by referencing the following equations and example strain rosette in Figure 30.

$$\varepsilon_x = \varepsilon_a$$
$$\varepsilon_y = \varepsilon_c$$
$$\gamma_{xy} = 2\varepsilon_b - \varepsilon_c - \varepsilon_a$$
$$\sigma_x = \frac{E}{1-\nu^2}\left(\varepsilon_x - \nu\varepsilon_y\right)$$
$$\sigma_y = \frac{E}{1-\nu^2}\left(\varepsilon_y - \nu\varepsilon_x\right)$$
$$\tau_{xy} = \gamma_{xy} G$$

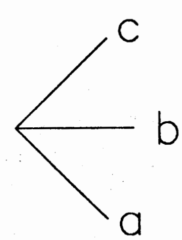

Figure 30. Example Strain Rosette and Useful Equations

The calculations of the stresses for one rosette are shown below and all values are shown in Table 6 and 7. The stresses are referenced to the stress block shown in Figure 31.

The Measured Strains

$\varepsilon_x = 389.5 \times 10^{-6}$

$\varepsilon_y = -62.5 \times 10^{-6}$

$\gamma_{xy} = [2(307.5) - 389.5 - (-62.5)] \times 10^{-6} = 288 \times 10^{-6}$

The Calculated Stresses

$\sigma_x = [(29E6)/(1-.3^2)][389.5E-6 + .3(-62.5E-6)] = 11.815$ ksi

$\sigma_y = [(29E6)/(1-.3^2)][-62.5E-6 + .3(389.5E-6)] = 1.732$ ksi

$\tau_{xy} = (288E-6)(11.3E6) = 3.2544$ ksi

TABLE 6

CALCULATED STRESSES FOR ORIGINAL DETAIL

Rosette	σ_x	σ_y	τ_{xy}
1	14.13	9.61	6.95
2	4.26	7.61	4.25
3	-4.09	1.42	-0.96

TABLE 7

CALCULATED STRESSES WITH BOLTS REMOVED

Rosette	σ_x	σ_y	τ_{xy}
1	11.72	1.50	3.25
2	16.95	15.38	7.06
3	-12.34	-1.53	-2.68

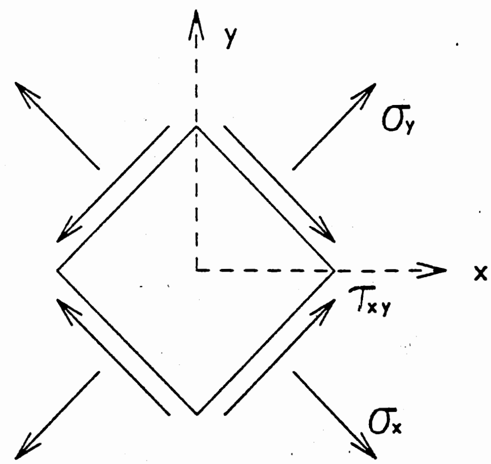

Figure 31. The Referenced Stress Block

The stresses corresponding to the referenced stress block can be used to calculate the principal stresses. The principal stresses for one rossette are calculated below and the other values are shown in Table 8 and 9.

The Principal Stresses

$$\sigma_{1,2} = \frac{11.815 + 1.732}{2} \pm \sqrt{\left(\frac{11.815 - 1.732}{2}\right)^2 + \tau_{xy}^2}$$

$$\sigma_1 = 12.78 \text{ ksi} \qquad \sigma_2 = 0.78 \text{ ksi}$$

The Angle of Rotation

$$\text{Tan } 2\theta_p = \frac{2(3.254)}{2}$$

$$\theta_p = 16.42^\circ$$

TABLE 8

PRINCIPAL STRESSES FOR ORIGINAL DETAIL

Rosette	σ_1 ,ksi	σ_2,ksi	θ_P ,degrees
1	19.18	4.56	36.0
2	10.51	1.36	-34.2
3	1.59	-4.25	9.6

TABLE 9

PRINCIPAL STRESSES WITH BOLTS REMOVED

Rosette	σ_1 ,ksi	σ_2,ksi	θ_P ,degrees
1	12.67	0.56	16.3
2	23.27	9.07	41.8
3	-0.91	-12.97	13.2

APPENDIX D

CAPACITY OF CONNECTION WITH BOLTS REMOVED

The loading from an H20 truck is shown in Figure 32. For the worst case, the connection will be checked to insure it can withstand the entire rear axle load.

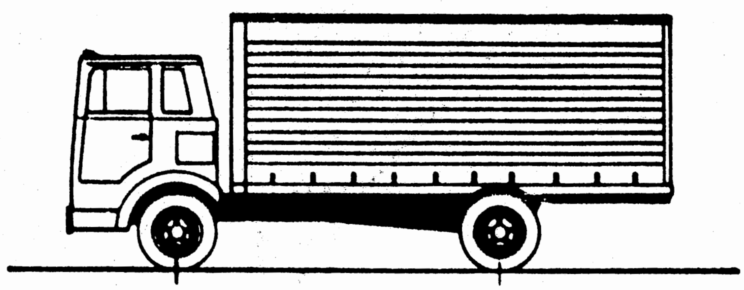

Figure 32. Loading for an H Truck

Check for Shear Strength

Capacity = $\Phi F_v A_b n$ = (0.65)(54 ksi)(0.4418)5

Capacity = 77.5 k > 51.2 k = (1.6)(32 k)

Check for Bearing Strength

Capacity = ΦR_n = (0.75)(2.4)(0.75)(0.25)(36 ksi)5

Capacity = 60.75 k > 51.20 k = (1.6)(32 k)

The checks were made using the LRFD specification (10). The connection with the two lower bolts removed has enough capacity.

VITA

Adam B. West

Candidate for the Degree of

Master of Science

Thesis: MODIFICATION OF FATIGUE DAMAGED STEEL BRIDGE DIAPHRAGMS

Major Field: Civil Engineering

Biographical:

Personal Data: Born in Stuart, Oklahoma, March 17, 1965, the son of Ronald West and Leonda Shields.

Education: Graduated from Stuart High School, Stuart, Oklahoma, in May 1983; received Bachelor of Science degree in Civil Engineering from Oklahoma State University in May, 1988; completed requirements for the Master of Science degree at Oklahoma State University in July, 1989.

Professional Experience: Research Assistant, Department of Civil Engineering, Oklahoma State University, May, 1988, to May, 1989. Teaching Assistant, College of Engineering, Oklahoma State University, August, 1987 to May, 1988. Research Assistant, Department of Civil Engineering, Oklahoma State University, June, 1987 to August, 1987.

Professional Organizations: American Society of Civil Engineers, American Concrete Institute, National Society of Professional Engineers, Oklahoma Society of Professional Engineers.